A Herschel telescope background model for the PACS photometer

U. Klaas[1]

[1] **Max-Planck-Institut für Astronomie,**
Königstuhl 17, D-69117 Heidelberg, Germany

Change Record

Version	Date	Changes	Remarks
Issue 1.0	09-May-2016	–	New document
Issue 1.1	17-May-2016	Intro, sect. 2.2 Fig. 12 y-axis scaling	Comments by Th. Müller included
Issue 1.2	23-May-2016	New sect. 6 Discussion of red background level discrepancy in sect. 5 Discussion on origin of extra red background in sect. 3.1.3 More detailed description of jump between blue and red spectrometer model part in sect. 3.1.1	Feedback from A. Poglitsch
Issue 1.3	June 27, 2016	Additional Fig. 7 & Table 1 showing cryostat thermal components for analysis of origin of extra red background and correction of text in sect. 3.1.3	Adaptation of discussion of extra red background
		Additional reference wrt. red bolometer signal level discussion in sect. 5	Adaptation of info on red bolometer signal level

Contents

1 Introduction **4**

2 First stage model based on the analytical SPIRE model **4**

2.1 Evolution of the telescope mirror temperatures 4

2.2 Emissivity change of primary mirror 6

2.3 Stage 1 of the telescope background model 7

3 Comparison with the PACS spectrometer telescope background model **7**

3.1 Adaptation of the PACS photometer background model 9

3.1.1 Compensation of the flux step in the spectrometer background model 9

3.1.2 Progressive amount of Rayleigh scattering 9

3.1.3 Additional "red" background 9

3.2 Verification of the adapted PACS photometer background model 11

4 Final PACS photometer background model **14**

5 OD dependent telescope background power for the three PACS photometer bandpasses **15**

6 Application of the telescope background model: Correlation of detector responsivity variations with telescope background variation **17**

7 Summary **17**

8 References **18**

9 Appendix: OD dependent telescope background power for the three photometer bandpasses **19**

1 Introduction

The derivation of an analytical Herschel telescope background model covering the whole PACS photometer wavelength range is described. It allows to take into account temperature and emissivity variations of the telescope system with a time resolution of individual ODs/OBSIDs.

2 First stage model based on the analytical SPIRE model

Hopwood et al. (2014) describe a Herschel telescope emission model based on the primary and secondary mirror temperature and the laboratory absorptivity measurements of Herschel telecope mirror coatings by Fischer et al. (2004):

$$Bg_{\rm tel}(\lambda) = (1-\varepsilon_{\rm M2}(\lambda))\,\varepsilon_{\rm M1}(\lambda)\,B_\nu(T_{\rm M1},\lambda) + \varepsilon_{\rm M2}(\lambda)\,B_\nu(T_{\rm M2},\lambda) \qquad [MJysr^{-1}] \tag{1}$$

with the wavelength dependent mirror emissivities of a dusty mirror sample

$$\varepsilon_{\rm M1}(\lambda) = \varepsilon_{\rm M2}(\lambda) = 0.0336\,\lambda^{-0.5} + 0.273\,\lambda^{-1} \qquad (\lambda\ in\ \mu m) \tag{2}$$

and the Planck function

$$B_\nu(T,\lambda) = \frac{2\,h\,c}{\lambda^3}\,\frac{1}{e^{\frac{h\,c}{k\,T\,\lambda}}-1} \tag{3}$$

2.1 Evolution of the telescope mirror temperatures

The Herschel primary and secondary mirror temperatures were not constant, but showed a superpositon of seasonal variation due to different distance to and hence illumination by the Sun and steady variations due to the initial cool-down and the following equilibration and afterwards changes in the emissivity and scattering properties of the mirrors along the mission. Fig. 1 shows the mirror temperatures measured for all ODs, when the PACS photometer was switched on. The primary mirror was warmer than the secondary mirror which was farther out in space. The minimum in mirror temperature was on OD 64 when the initial in-orbit cool-down trend was reverted into a relatively steep temperature increase with gradual equilibration at around OD 300.

In Fig. 2 the seasonal variations and gradual changes after OD 290 are high-lighted by fitting by eye the following functions

$$T_{\rm M1}^{fit} = 88.7\ [K] - 0.6\ [K]\ sin(\frac{OD}{182.62}\,\pi + 0.2\,\pi) + 0.6\ [K]\ \frac{OD-290}{1160} \tag{4}$$

$$T_{\rm M2}^{fit} = 84.7\ [K] - 0.5\ [K]\ sin(\frac{OD}{182.62}\,\pi + 0.2\,\pi) \tag{5}$$

Visible dips and enhancements relative to the fit can be explained by the distribution of attitudes of the telescope wrt. solar angle. A phase with many "cold" attitudes led to a dip, a phase with a larger number of "warm" attitudes to an enhancement of the mirror temperatures. Minima of the seasonal variations are at OD 420 (07-Jul-2010), OD 785 (07-Jul-2011), and OD 1151 (07-Jul-2012), which is close in time to Earth at aphelion (farthest distance from the Sun) and maxima of the seasonal variations are at OD 603 (06-Jan-2011), OD 968 (06-Jan-2012) and OD 1334 (06-Jan-2013), which is close in time to Earth at perihelion (closest distance from the Sun). The amplitude of the seasonal variation is ±0.6 K for the primary mirror and ±0.5 K for the secondary mirror.

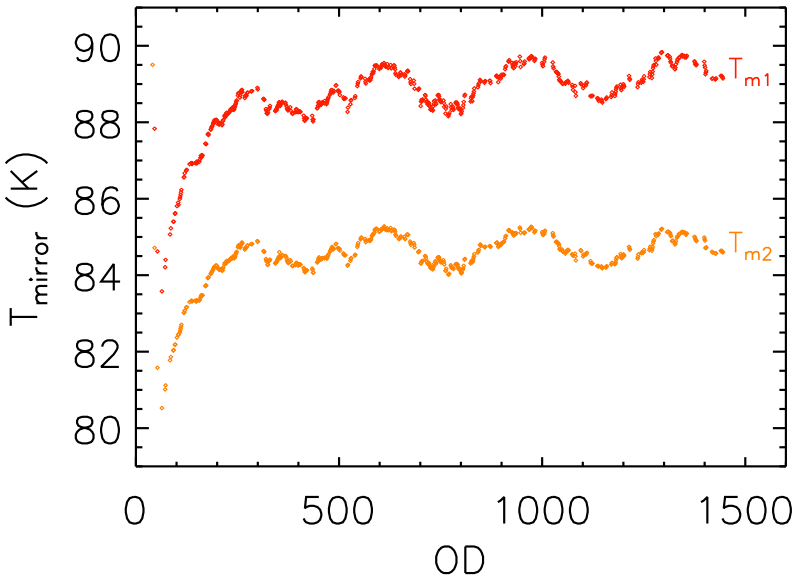

Figure 1: Temperature evolution of the primary (m1) and secondary (m2) Herschel telescope mirrors over the mission. Average temperatures per OD from all measurements associated with PACS photometer measurements.

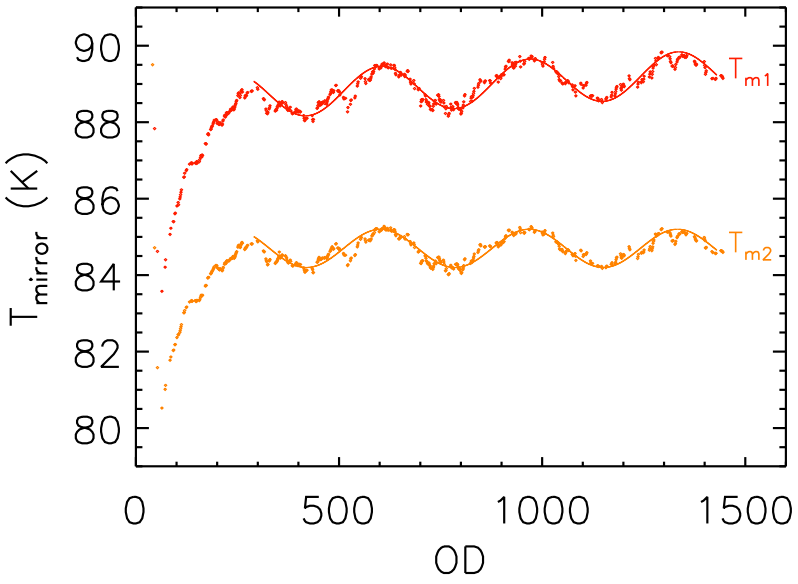

Figure 2: Temperature evolution of the primary (m1) and secondary (m2) Herschel telescope mirrors over the mission. Seasonal variations and gradual trends after OD 290 have been fitted by eye as described in Eqs. 4 and 5.

The trend fit also shows, that the average temperature of the secondary mirror remains at 84.7 K, while the average temperature of the primary mirror increases by 0.6 K from 88.7 K to 89.3 K.

The steady increase of the temperature difference between primary and secondary mirror and the effect of the 0.1 K higher seasonal amplitude of the primary mirror is shown in Fig. 3.

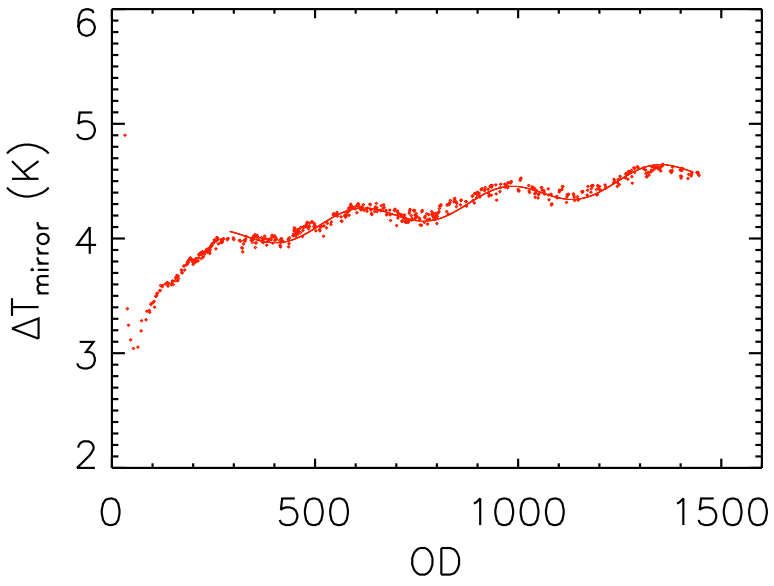

Figure 3: Evolution of the temperature difference between primary (m1) and secondary (m2) Herschel telescope mirrors over the mission. The steady increase and the seasonal amplitude of ±0.1 K are all related to the stronger variations of the primary mirror.

2.2 Emissivity change of primary mirror

The trend fits in Eq. 5 and Eq. 4 describing a constant average temperature of M2 and a steady temperature increase for M1 lead to the conclusion that the secondary mirror does not change its emission properties, while the primary does. The increase of the average primary mirror temperature is measured between OD 329, $T_{M1}(\mathrm{OD}\,329) = 88.38\,\mathrm{K}$, and OD 1426, $T_{M1}(\mathrm{OD}\,329) = 89.12\,\mathrm{K}$, as $\Delta T = 0.74\,\mathrm{K}$. The relative change in emissivity is estimated, assuming equal flux for two blackbodies with these two slightly different temperatures

$$|\Delta\,\varepsilon| = 1.0 - \frac{B_\nu(T_{ini}, \lambda)}{B_\nu(T_{fin}, \lambda)} \tag{6}$$

This gives a relative change of 1.3% (160µm) ... 2.1% (70µm), which is in the order of the maximum emissivity correction derived by Hopwood et al. (2014).

The emissivity of the primary mirror is therefore described as

$$\varepsilon_{M1}(\lambda) = \begin{cases} 0.0336\,\lambda^{-0.5} + 0.273\,\lambda^{-1} & : \quad for\ OD < 290 \\ (1.0 + 0.02\,\frac{OD-290}{1160}) \times (0.0336\,\lambda^{-0.5} + 0.273\,\lambda^{-1}) & : \quad for\ OD \geq 290 \end{cases} \tag{7}$$

2.3 Stage 1 of the telescope background model

Fig. 4 shows the first stage of the telescope background for the whole PACS photometer wavelength range based on Eqs. 1, 2, 3, and 7.

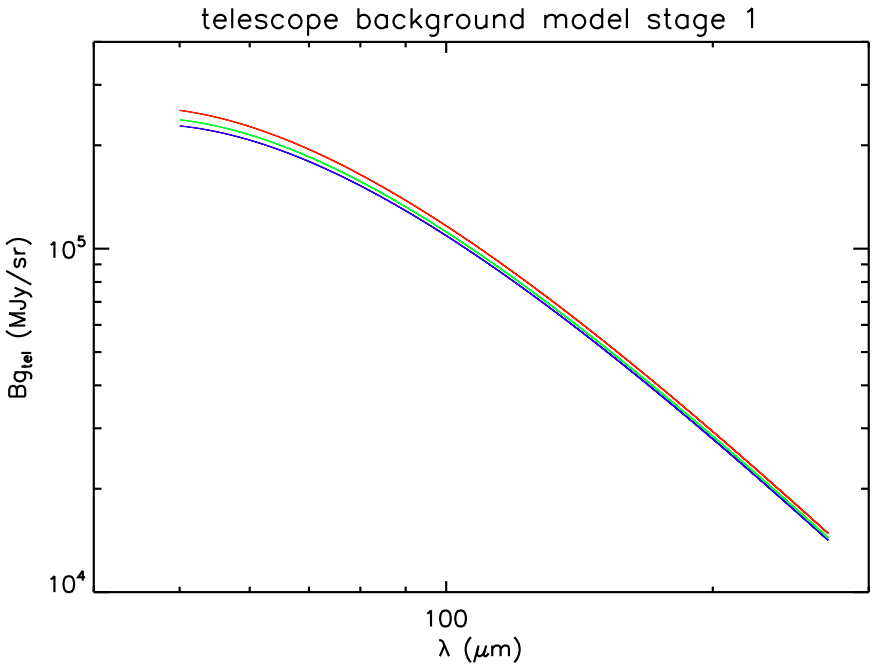

Figure 4: First stage of the telescope background model considering the emission of the two telescope mirrors with a wavelength dependent emissivity and an aging of the primary mirror emissivity. Blue: background on OD 132 (first photometer OD with final bias setting on steep mirror temperature rise); green: background on OD 415 (first seasonal minimum after thermal equilibration of mirrors with little aging); red: background on OD 1344 (last seasonal maximum with close to full aging effect of primary mirror).

3 Comparison with the PACS spectrometer telescope background model

For further upgrade of the photometer background model a comparison and adjustment with the PACS spectrometer model is performed. The spectrometer model is absolutely calibrated by Pallas and Ceres spectra and the temporal evolution is derived from many measurements of the secondary flux standard HD 161796 at the key wavelengths 60, 75, 120, 150, and 180 µm (Poglitsch 2015). The model is stored in the calibration file PCalSpectrometer_TelescopeBackground_FM_v8.fits. The comparison is concentrated on the period OD 290 to end of mission with the smooth and periodic temperature evolution, ODs 415 and 1344 with the most separated seasonal minimum and maximum are selected. With regard to wavelength comparison the spectrometer background model is restricted to the wavelength range 55 . . . 190 µm with a gap between 101 and 103 µm. The spectrometer background model is expressed in Jy/spaxel, therefore the photometer model is converted

$$F_{\rm tel}(\lambda) = \Omega\, Bg_{\rm tel}(\lambda) \qquad [Jy] \tag{8}$$

with $\Omega = 2.0769\,10^{-9}$ sterad for a square 9.4”×9.4” spectrometer spaxel (spatial pixel).

Fig. 5 shows the comparison of the stage 1 PACS photometer background model with the empirical (solely

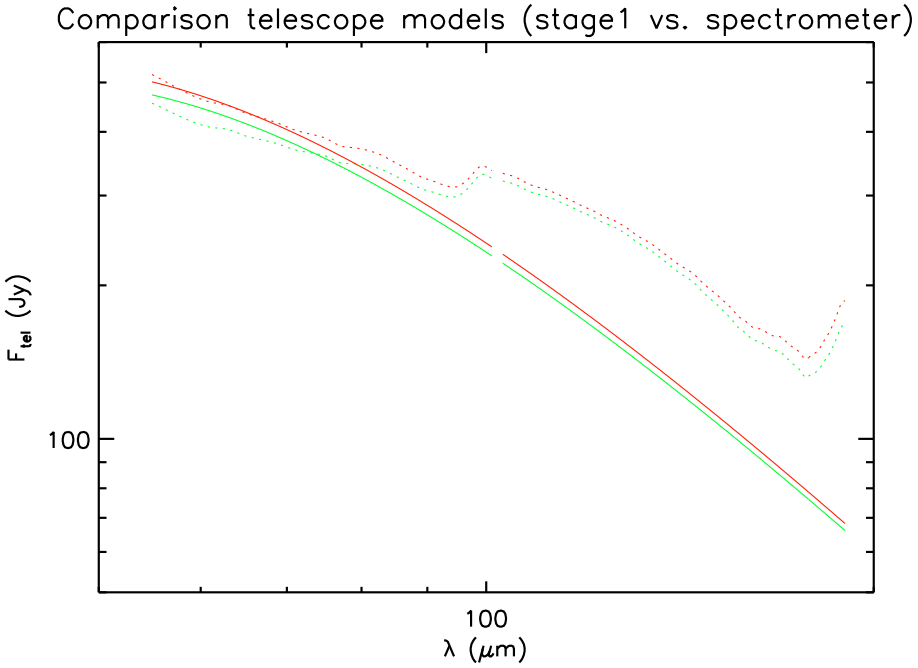

Figure 5: Comparison of stage 1 PACS photometer background model (solid lines) with the PACS spectrometer background model (dashed lines). Green: background on OD 415; red: background on OD 1344.

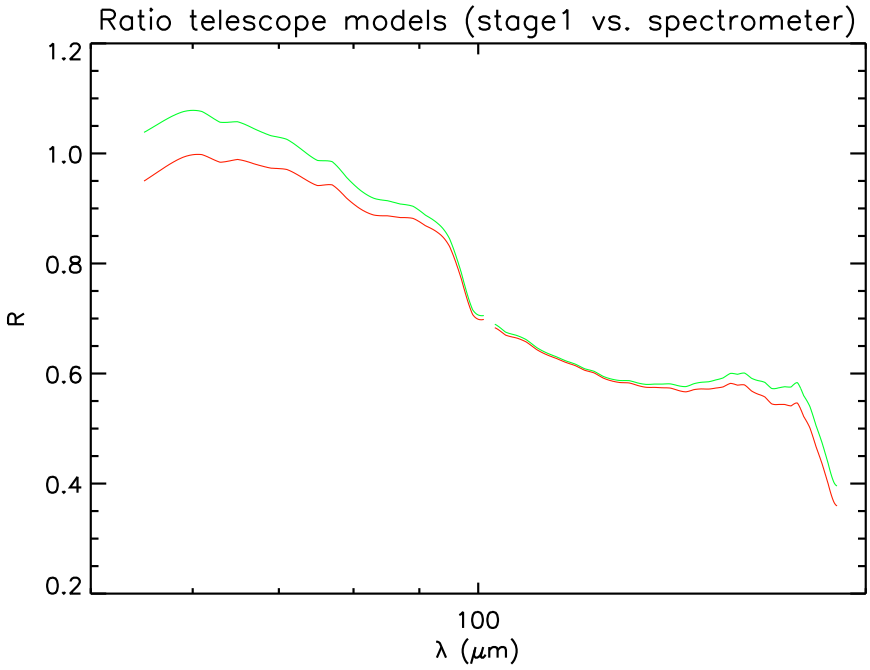

Figure 6: Ratio of stage 1 PACS photometer background model and PACS spectrometer background model. Green: background on OD 415; red: background on OD 1344.

based on measurements) PACS spectrometer model for the two selected ODs, Fig. 6 the respective ratios. It can be seen that for the shortest wavelengths the absolute levels are quite consistent. It is noted that the

two spectrometer curves are more spread up to 100 µm. This behaviour is associated to temporal evolution in Rayleigh scattering on the primary mirror. The temporal evolutions for the long wavelength part are quite the same for both models, however the photometer model is only on the 60% level. It has to be pointed out, that this discrepancy is in reality considerably smaller, since the flux step in the spectrometer telescope model between about 94 and 99µm is not a real background feature, but due to the fact that instrumental effects are implicitly corrected for (accounting for different responses of blue and red detectors). Nevertheless it is clear that an additional cold emission component (an extra "red" background) is needed to better match the two models.

3.1 Adaptation of the PACS photometer background model

3.1.1 Compensation of the flux step in the spectrometer background model

As pointed out in the previous section, the jump between blue and red part of the spectrometer background model can be associated to different time constants of the blue and red spectrometer detectors. The telescope is measured in DC mode, but the signal is chopped (AC mode), which has the impact that the faster blue detector sees more of the modulation than the slower red one. For that reason the telescope appears brighter to the red detector compared to the blue detector. Because of the good correspondence of the stage 1 model with the blue part in the 55 – 70 µm region, we adopt the absolute levels in the blue part as 1:1. A factor of $\mathrm{fac}_{sl} = 1.22$ is multiplied to the 103–190 µm part of the PACS photometer model to compensate for the flux step in the spectrometer model.

3.1.2 Progressive amount of Rayleigh scattering

The spread between background curves from early and late mission closing at around 100 µm can be well modelled by by a strongly inverse wavelength dependent term. A Rayleigh scattering term of the form

$$\sigma_{\mathrm{Rayleigh}} = \begin{cases} 0. & : \quad for\ OD < 290 \\ (1.0 + 340.0\,\frac{OD-290}{1160}) \times \frac{50.}{\lambda^4} \quad (\lambda\ in\ \mu m) & : \quad for\ OD \geq 290 \end{cases} \tag{9}$$

was added to the primary mirror emissivity term $\varepsilon_{\mathrm{M1}}$ (cf. Poglitsch 2012).

3.1.3 Additional "red" background

The additional red background is modelled by a modified blackbody which has to contribute noticable longward of 70 µm, i.e. has to be considerably colder than 43 K (BB peaking at 70 µm). Since the additional red background is noticable already at 70 µm, it is concluded that this thermal component has its origin outside the PACS instrument and is present both in the PACS photometer and spectrometer optical trains.

A quite good correspondence with the spectrometer model is achieved with a 22 K black body with emissivity $\propto \lambda^{-2}$. An emissivity $\propto \lambda^{-1}$ gives a too flat decline and does not match at all the bent in the spectrometer background model longward of 136 µm. An emissivity $\propto \lambda^{-2.5}$ would even provide a somewhat better match.

$$Bg_{\mathrm{extrared}} = \frac{3.2\,10^3}{\lambda^2}\, B_\nu(22\,K, \lambda) \tag{10}$$

The orgin of this extra "red" component is unclear. Checking the S/C temperature sensor housekeeping telemetry of the payload module components (cf. Fig. 7 and Table 1), there is one component with approximately this temperature, namely $\mathrm{T_{HOT}}$, which is the auxilliary HeI tank. However, this auxilliary HeI tank is located at the bottom of the prime HeII tank on the opposite side of the 12 – 13 K cold optical bench, which carries the instruments and is covered by the instrument shield with the same temperature. It appears unlikely that the 22 K component can be explained by stray-light generated by emission from the HOT.

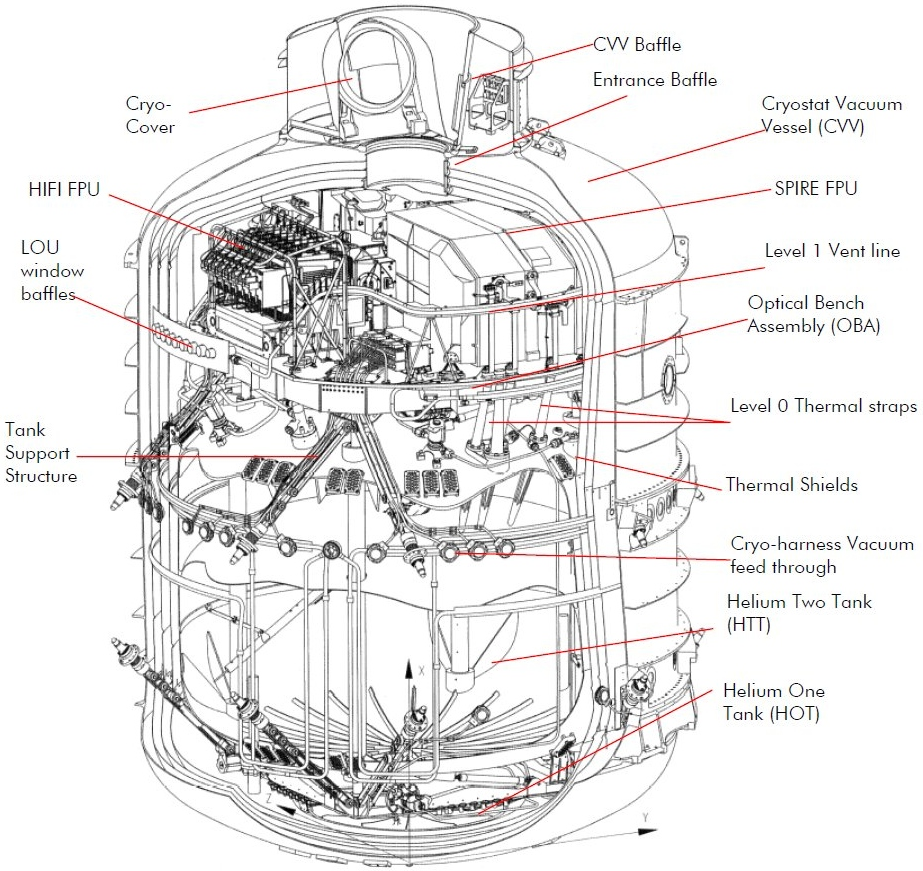

Figure 7: Cross-sectional view of the Herschel payload module showing the main components of the cryogenic system (from Herschel Handbook).

Table 1: Temperature ranges of thermal components of the Herschel cryostat.

thermal component	temperature range (K)
Optical bench	11.5 – 13.5
Instrument shield	11.5 – 13.5
Cryostat baffle	74.0 – 76.5
Cryostat shield 1	36.5 – 38.5
Cryostat shield 2	49.0 – 50.5
Cryostat shield 3	60.0 – 62.0
HOT (HeI tank)	21.0 – 22.0

3.2 Verification of the adapted PACS photometer background model

Fig. 8 shows the comparison with the spectrometer model after implementing the three adaptation items. As the ratio in Fig. 9 shows, the correspondence is quite good over a large wavelength range and better than 10% for all wavelengths except at the very end of each part, where the spectrometer is affected by leakage of higher orders. For the shortest wavelengths the spectrometer model has a slightly flatter shape. No attempt has been made to adapt the photometer model in absolute flux for the short wavelengths.

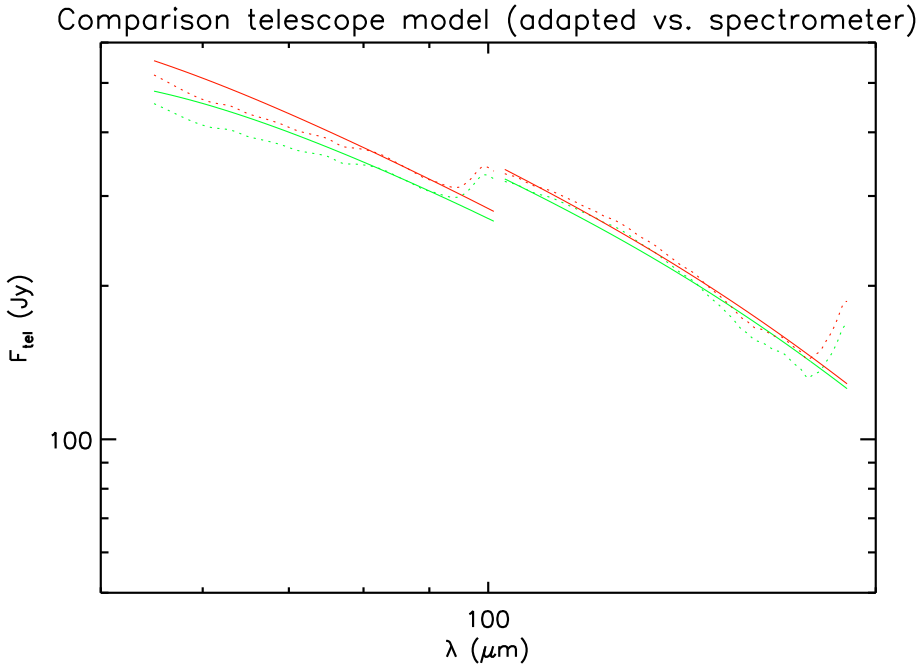

Figure 8: Comparison of adapted PACS photometer background model (solid lines), as described in Sect. 3.1, with the PACS spectrometer background model (dashed lines). Green: background on OD 415; red: background on OD 1344.

The adaptation of the photometer model was optimized for the combination of the ODs 415 and 1344. One difference between photometer model and spectrometer model is that the temporal evolution applied here starts from OD 290 (when the secondary mirror is considered in a temperature equilibrium except of the seasonal variations), while the spectrometer model determined an evolution from OD 200 onwards, when the equilibration does not appear to have finished. Figs. 10 and 11 show a verification for the whole OD range from OD 200 to OD 1445 with intermediate ODs 611 and 1028. There is some scatter in the ratio, but this is within an acceptable range.

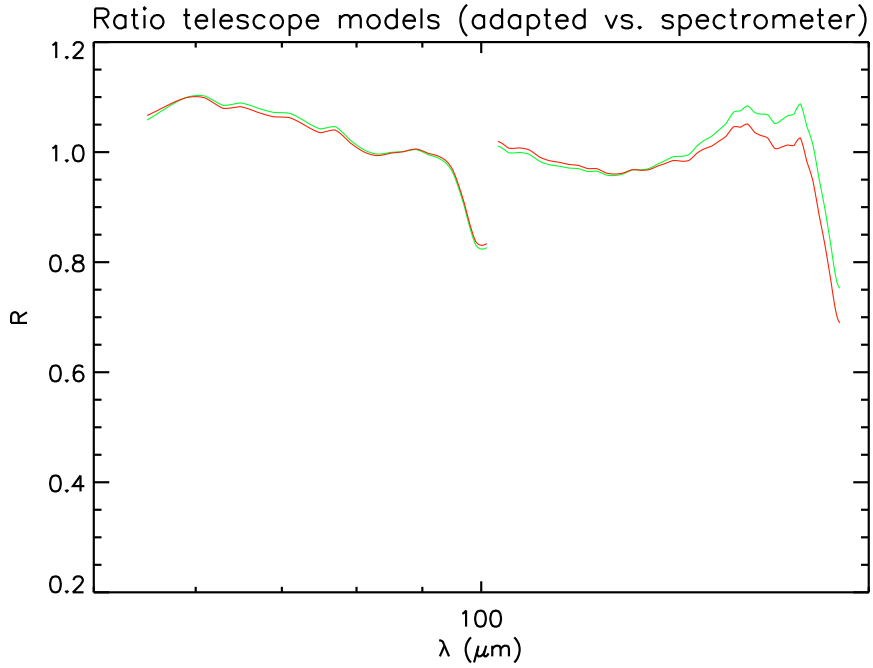

Figure 9: Ratio of adapted PACS photometer background model, as described in Sect. 3.1, and PACS spectrometer background model. Green: background on OD 415; red: background on OD 1344.

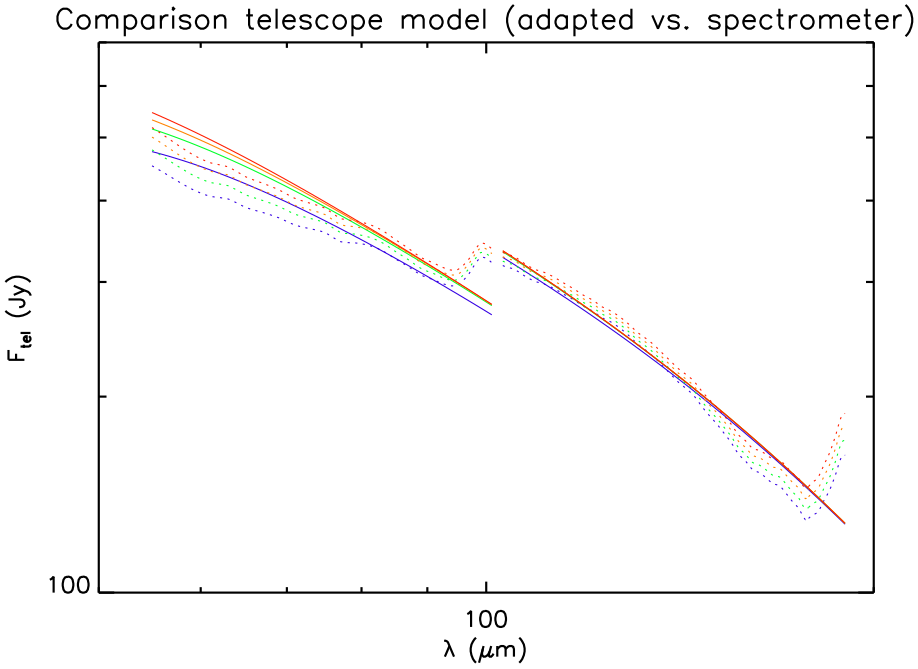

Figure 10: Verification of adapted PACS photometer background model (solid lines), as described in Sect. 3.1, with the PACS spectrometer background model (dashed lines) for more ODs. Blue: background on OD 200; green: background on OD 611; orange: background on OD 1028; red: background on OD 1445.

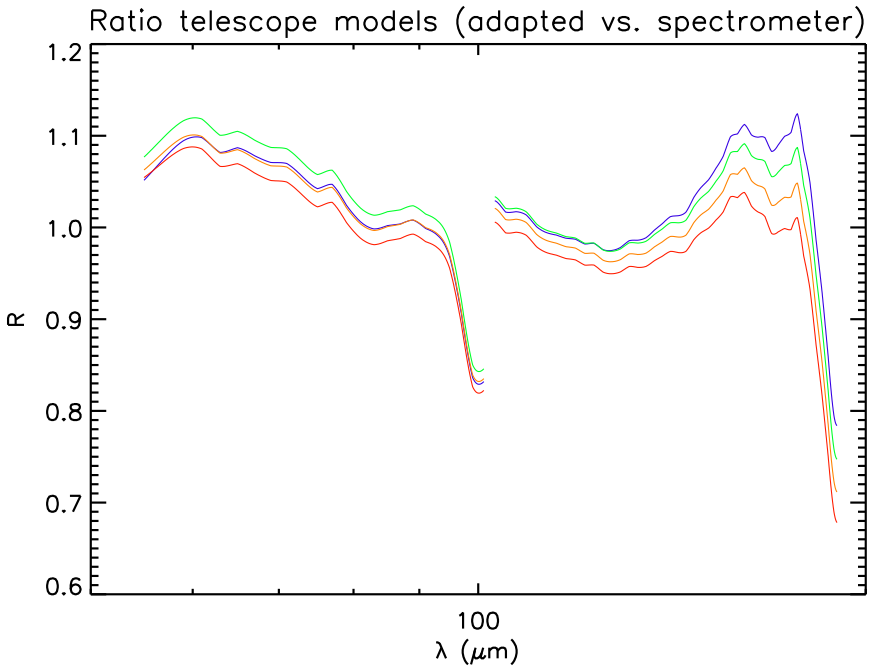

Figure 11: Verification of the ratio of adapted PACS photometer background model, as described in Sect. 3.1, and PACS spectrometer background model for more ODs. Blue: background on OD 200; green: background on OD 611; orange: background on OD 1028; red: background on OD 1445.

4 Final PACS photometer background model

The final telescope background model for the PACS photometer is described by

$$Bg_{\rm tel}(\lambda, OD/OBSID) = [1-\varepsilon_{\rm M2}(\lambda)]\,[\varepsilon_{\rm M1}(\lambda, OD) + \sigma_{\rm Rayleigh}(\lambda, OD)]\,B_\nu(T_{\rm M1}(OD/OBSID), \lambda) + \varepsilon_{\rm M2}(\lambda)\,B_\nu(T_{\rm M2}(OD/OBSID), \lambda) + Bg_{\rm extrared}(\lambda) \quad [MJy\,sr^{-1}] \quad (11)$$

with $\varepsilon_{\rm M2}(\lambda)$ from Eq. 2, $\varepsilon_{\rm M1}(\lambda, OD)$ from Eq. 7, $\sigma_{\rm Rayleigh}(\lambda, OD)$ from Eq. 9, and $\rm Bg_{extrared}$ from Eq. 10. $\rm B_\nu(T_{M1,2}(OD, OBSID), \lambda)$ is the Planck function, as defined in Eq. 3. The telescope mirror temperatures $\rm T_{M1}(OD/OBSID)$ and $\rm T_{M2}(OD/OBSID)$ are either the average ones per OD as given in Sect. 9 or even the ones for the individual observation ID (OBSID).

Fig. 12 shows the final telescope background model for the whole PACS photometer wavelength range based on Eq. 11.

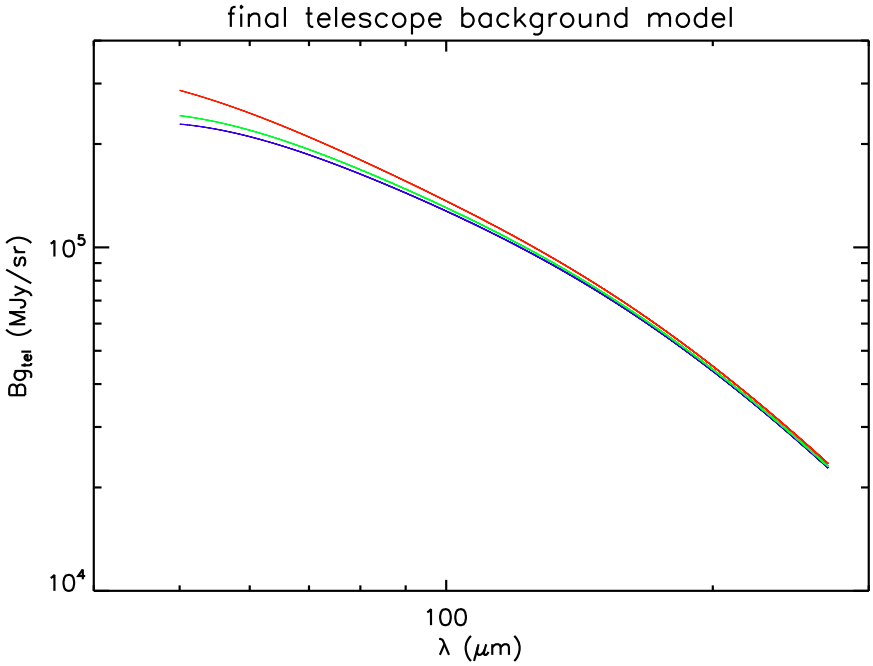

Figure 12: Final PACS photometer telescope background model considering the emission of the two telescope mirrors with a wavelength dependent emissivity and an aging of the primary mirror emissivity plus progressive Rayleigh scattering and a constant extra "red" background. Blue: background on OD 132 (first photometer OD with final bias setting on steep mirror temperature rise); green: background on OD 415 (first seasonal minimum after thermal equilibration of mirrors with little aging); red: background on OD 1344 (last seasonal maximum with close to full aging effect of primary mirror).

5 OD dependent telescope background power for the three PACS photometer bandpasses

For a calibration assessment of the bolometer responsivity dependence on the telescope background the total power of the telescope background per pixel in each photometer bandpass is computed as

$$P_{\rm tel}(OD/OBSID) = A_{\rm eff}\, T_{\rm refl} \int_{\lambda_1}^{\lambda_2} \frac{c}{\lambda^2}\, R(\lambda)\, \Omega_{\rm pix}\, Bg_{\rm tel}(\lambda, OD/OBSID)\, d\lambda \qquad (pW) \qquad (12)$$

with effective primary mirror area $A_{\rm eff} = 8.709\,{\rm m}^2$ (as in PACS responsivity cal file), $T_{\rm refl} = 0.99^{14} = 0.869$ (14 mirrors reflection inside PACS photometer), the bandpass response $R(\lambda)$ between wavelengths λ_1 and λ_2, the solid angle $\Omega_{\rm pix}$ (3".2 pixel size for blue and green band, 6".4 pixel size for red band) and the final telescope background model per photometer OD or OBSID $Bg_{\rm tel}(\lambda, OD/OBSID)$.

Fig. 13 shows the calculated evolution of the telescope background power per pixel with OD for the three photometer bandpasses, Fig. 14 a zoomed view for each bandpass individually. A table with the values is given in the appendix.

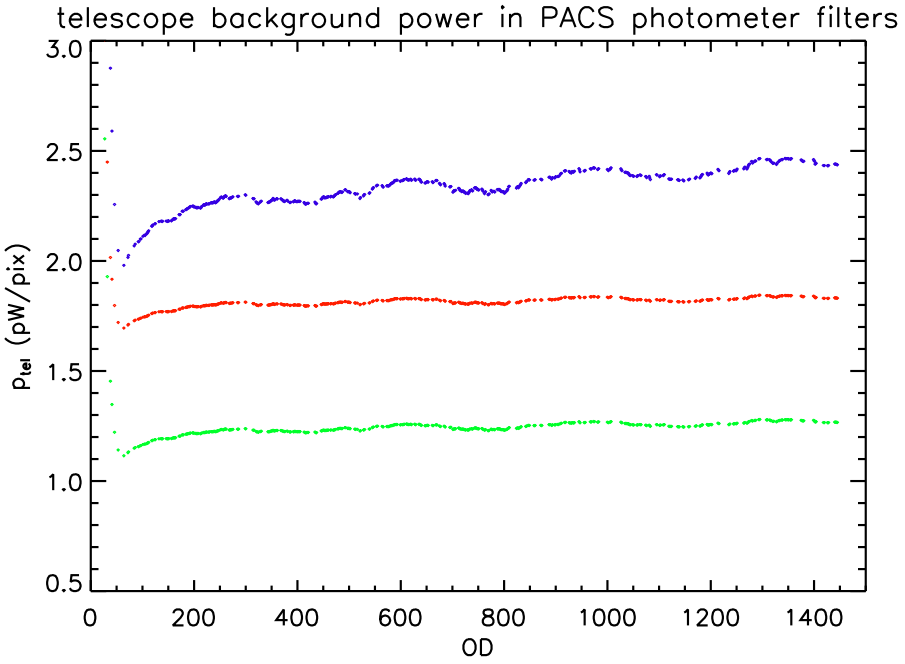

Figure 13: Evolution of the telescope background power per pixel with OD for the three photometer bandpasses computed according to Eq. 12. Blue: 70 µm band; green: 100 µm band; red: 160 µm band (note that the red detector pixel has a 4 times larger solid angle than the blue detector pixel).

We note that for the 160 µm band the background should be of the order 4 pW. This is based on the comprehensive on-ground ILT photometer flux calibration, which related the detector output signals to the calibrated infalling flux in the range 0 – 7 pW. It was noted already early in the Herschel mission that there is a discrepancy in the order of ≈2 pW between telescope background predictions and the actual background flux level in the red band (see e.g. Sauvage et al. 2009 and Sauvage 2009). Based on the comparison with the PACS spectrometer background model, there is no indication for such a large extra background in the 160 µm band coming from the telescope/common optics system. Also there is a good correspondence between the in-band power levels and the model background power predictions for the 70 µm and 100 µm filters. The discrepancy is solely related to the red photometer detector and it is suspected that the extra (stray-)light could be related to emission caused

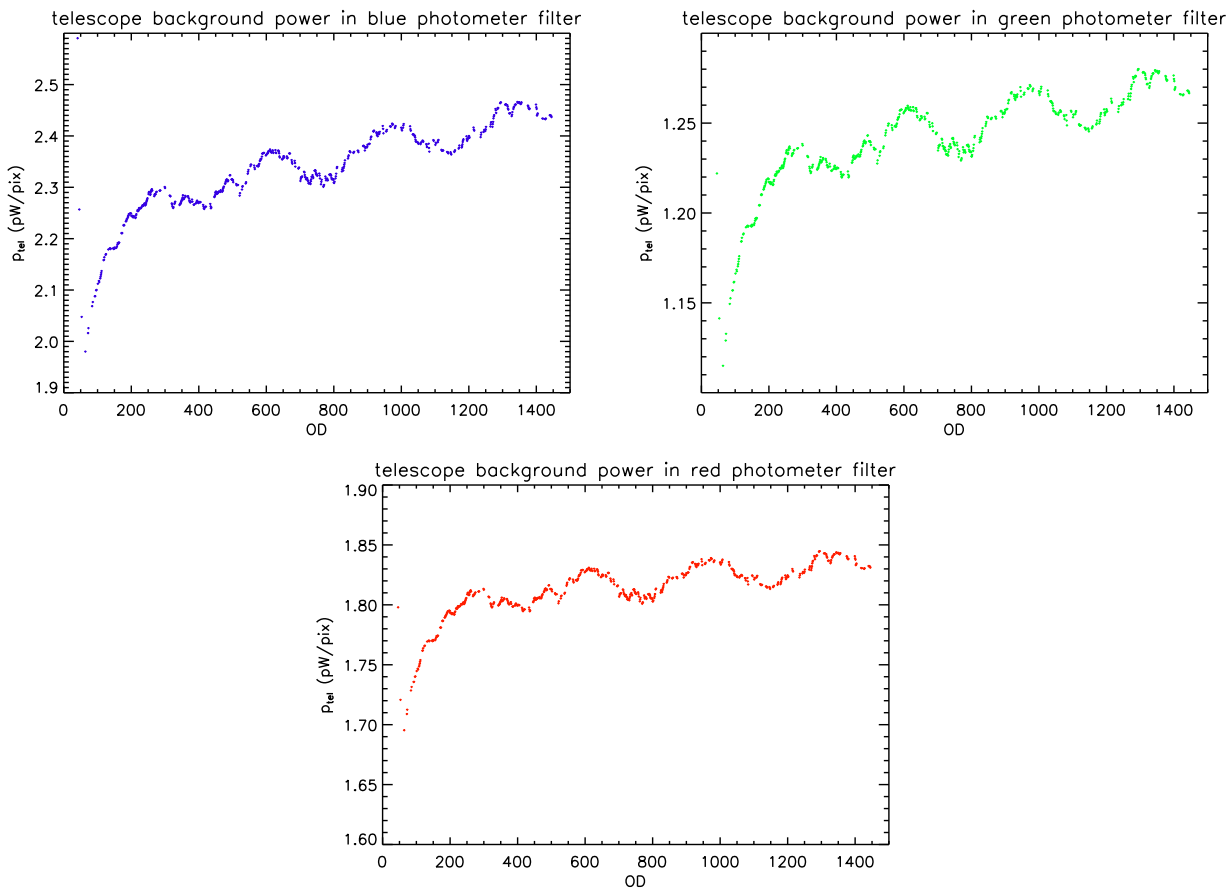

Figure 14: Zoomed view of the evolution of the telescope background power per pixel with OD for each individual photometer bandpass. Top left: 70 µm band; top right: 100 µm band; bottom: 160 µm band.

by the close-by read-out electronics (see discussion in Sauvage et al. 2009), but the exact origin of the source remains unknown.

6 Application of the telescope background model: Correlation of detector responsivity variations with telescope background variation

The main application of the photometer background model is the investigation whether the variations of the telescope background are large enough that systematic variations of the bolometer responsivities can be recognized.

Fig. 15 shows clear correlations between the measured/model flux ratio and the predicted telescope background power at the times of observation established for the five PACS fiducial standard stars in the 70 and 100 µm filters. The flux ratio is a measure of the responsivity variation. It should be noticed that the measured fluxes have been corrected beforehand for another responsivity variation caused by the variation of the PACS cooler evaporator temperature. For the 160 µm filter the systematic variation is less than 0.1% and not detectable taking into account the error bars.

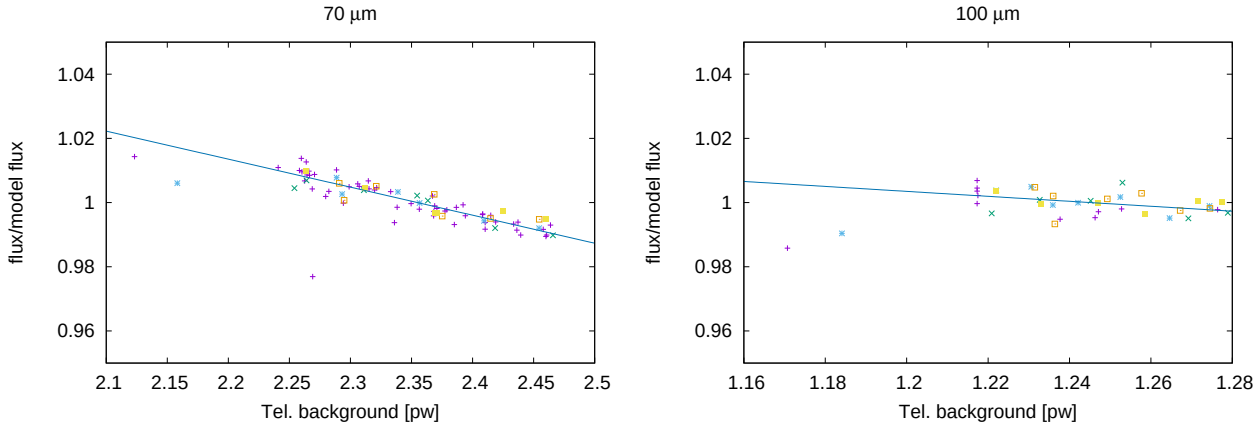

Figure 15: Correlation of the ratio measured/model flux for the PACS photometer fiducial standard stars with the estimated telescope background power at the time of observation for the 70 and 100 µm filters. The fluxes of the standard stars have been corrected before for responsivity effects with the evaporator temperature.

The effect of varying telescope background is largest for the 70 µm filter, with a variation of the detector responsivity of ∼2.23% for 0.25 pW background variation. For the 100 µm filter the detector responsivity variation amounts to only ∼0.46% for 0.06 pW background variation. This is in very good agreement with the pre-flight ground calibration non-linearity assessment (Billot & Okumura 2008) over the background power range 0 – 7 pW, which derived 1% of responsivity loss for ≈0.1 pW/pixel flux increase.

7 Summary

This TN describes the establishment of a telescope background model per photometer OD on an analytical basis expressing the emission of the two Herschel telescope mirrors and implementing a number of aging effects, whose amplitudes are derived from mirror temperature sensor measurements and SED measurements with the PACS spectrometer. The model covers the full wavelength range of the three photometer bandpasses and allows to determine the in-band powers, which are relevant for assessment of detector responsivity changes with the telescope background level.

Acknowledgement: I thank Albrecht Poglitsch for his comprehensive work on the PACS spectrometer background model which provided a solid basis for setting up this TN for the PACS photometer background model.

8 References

- Billot, N.; & Okumura, K., 2008, PACS Test Analysis Report FM-ILT, req. 3.2.3 "Calibrate the photometer's non-linearity", http://pacs.ster.kuleuven.be/Documents/WBS/FMREP/065/001/FM_ILT_draft.pdf, p. 108
- Fischer, J.; Klaassen, T.; Hovenier, N.; Jakob, G.; Poglitsch, A.; Sternberg, O., 2004, Applied Optics Vol. 43, No. 19, 3765
- Hopwood, R.; Fulton, T.; Polehampton, E.T.; Valtchanov, I.; Benielli, D.; et al., 2004, Exp. Astronomy 37, 195
- Poglitsch, A., 2012, Telescope background model with aging, Telescope_BG_new_cal_alt.pdf
- Poglitsch, A., 2015, Description of telescope background (OD, λ), TelescopeSED-Calibrators.pdf
- Sauvage, M.; Okumura, K.; Billot N., 2009, SAp-PACS-MS-0707-09, Issue 1.0,"Instrument background determination and red-side signal level investigation", http://pacs.ster.kuleuven.be/Documents/WBS/FlightReports/016/001/BkgAndRedSignal_v1.0.pdf
- Sauvage, M., 2009, SAp-PACS-MS-0709-09, Issue 1.0, "Investigation of the impact of seasonal changes of the telescope temperature on the PACS photometer", http://pacs.ster.kuleuven.be/Documents/WBS/FlightReports/020/001/SeasonalEffectsPhot.pdf

9 Appendix: OD dependent telescope background power for the three photometer bandpasses

OD	70um (pW)	100um (pW)	160um (pW)	<T_m1> (K)	<T_m2> (K)
27	6.0403	2.5549	3.0049	137.967	129.857
32	4.2052	1.9290	2.4495	114.776	109.875
38	2.8761	1.4540	2.0160	96.813	93.425
41	2.5903	1.3480	1.9170	92.748	89.503
46	2.2569	1.2220	1.7980	87.833	84.716
53	2.0478	1.1414	1.7208	84.622	81.581
64	1.9803	1.1150	1.6954	83.578	80.525
72	2.0162	1.1291	1.7089	84.209	81.014
73	2.0259	1.1328	1.7126	84.402	81.119
84	2.0686	1.1494	1.7286	85.067	81.775
86	2.0767	1.1526	1.7315	85.228	81.861
92	2.0879	1.1569	1.7357	85.403	82.029
93	2.0882	1.1570	1.7358	85.399	82.043
96	2.0995	1.1614	1.7400	85.606	82.181
97	2.1004	1.1617	1.7403	85.625	82.190
101	2.1123	1.1663	1.7448	85.810	82.369
104	2.1178	1.1685	1.7468	85.900	82.448
105	2.1155	1.1676	1.7460	85.840	82.438
108	2.1226	1.1704	1.7486	85.995	82.499
109	2.1258	1.1716	1.7498	86.045	82.546
110	2.1295	1.1730	1.7511	86.104	82.601
111	2.1333	1.1745	1.7525	86.169	82.651
112	2.1372	1.1760	1.7540	86.231	82.706
118	2.1582	1.1841	1.7617	86.560	83.015
119	2.1588	1.1843	1.7619	86.570	83.022
120	2.1638	1.1862	1.7638	86.667	83.076
124	2.1685	1.1880	1.7655	86.734	83.153
125	2.1700	1.1886	1.7661	86.761	83.170
132	2.1790	1.1921	1.7694	86.904	83.299
136	2.1807	1.1927	1.7700	86.935	83.319
137	2.1814	1.1930	1.7703	86.937	83.338
138	2.1799	1.1924	1.7697	86.908	83.323
139	2.1806	1.1927	1.7699	86.930	83.320
146	2.1813	1.1930	1.7702	86.936	83.338
148	2.1800	1.1924	1.7697	86.922	83.310
149	2.1813	1.1929	1.7702	86.950	83.321
150	2.1829	1.1936	1.7708	86.975	83.345
151	2.1811	1.1929	1.7701	86.932	83.333
156	2.1824	1.1934	1.7706	86.968	83.336
157	2.1849	1.1943	1.7715	87.019	83.360
159	2.1884	1.1957	1.7728	87.074	83.413
160	2.1915	1.1969	1.7739	87.129	83.450
161	2.1918	1.1970	1.7741	87.111	83.478
162	2.1904	1.1965	1.7736	87.090	83.456
163	2.1928	1.1974	1.7744	87.145	83.472
164	2.1923	1.1972	1.7743	87.127	83.476
171	2.2107	1.2042	1.7810	87.441	83.714

OD	70um (pW)	100um (pW)	160um (pW)	<T_m1> (K)	<T_m2> (K)
172	2.2114	1.2045	1.7812	87.442	83.735
173	2.2108	1.2043	1.7810	87.429	83.729
177	2.2258	1.2100	1.7865	87.684	83.924
178	2.2270	1.2105	1.7869	87.703	83.942
179	2.2260	1.2101	1.7866	87.671	83.945
184	2.2337	1.2131	1.7894	87.809	84.037
185	2.2342	1.2133	1.7896	87.818	84.042
186	2.2364	1.2141	1.7904	87.859	84.066
187	2.2384	1.2148	1.7911	87.892	84.092
188	2.2393	1.2152	1.7914	87.901	84.112
190	2.2421	1.2163	1.7925	87.957	84.140
191	2.2444	1.2172	1.7933	87.992	84.173
192	2.2458	1.2177	1.7938	88.013	84.192
193	2.2481	1.2186	1.7946	88.054	84.222
197	2.2496	1.2192	1.7952	88.063	84.258
198	2.2497	1.2192	1.7952	88.069	84.253
199	2.2487	1.2188	1.7949	88.045	84.249
200	2.2444	1.2172	1.7933	87.970	84.196
203	2.2448	1.2173	1.7934	87.995	84.183
204	2.2423	1.2164	1.7925	87.947	84.156
205	2.2426	1.2164	1.7926	87.958	84.151
206	2.2416	1.2161	1.7923	87.943	84.138
207	2.2439	1.2170	1.7931	87.988	84.162
208	2.2433	1.2167	1.7929	87.965	84.166
212	2.2403	1.2156	1.7918	87.924	84.119
213	2.2413	1.2160	1.7922	87.951	84.121
214	2.2456	1.2176	1.7937	88.030	84.170
215	2.2478	1.2185	1.7945	88.061	84.205
218	2.2539	1.2208	1.7967	88.161	84.286
219	2.2559	1.2216	1.7975	88.187	84.321
220	2.2538	1.2207	1.7967	88.135	84.310
221	2.2544	1.2210	1.7969	88.161	84.301
222	2.2560	1.2216	1.7975	88.196	84.313
223	2.2593	1.2229	1.7987	88.247	84.363
224	2.2600	1.2231	1.7990	88.252	84.379
225	2.2583	1.2225	1.7983	88.209	84.369
228	2.2591	1.2228	1.7986	88.233	84.370
229	2.2601	1.2232	1.7990	88.258	84.374
230	2.2613	1.2236	1.7994	88.276	84.391
233	2.2650	1.2250	1.8008	88.342	84.436
234	2.2645	1.2248	1.8006	88.323	84.440
235	2.2641	1.2247	1.8004	88.316	84.435
236	2.2646	1.2249	1.8006	88.328	84.438
237	2.2655	1.2252	1.8010	88.349	84.444
238	2.2667	1.2257	1.8014	88.371	84.457
239	2.2688	1.2265	1.8021	88.401	84.489
240	2.2681	1.2262	1.8019	88.377	84.493
241	2.2650	1.2250	1.8008	88.324	84.454
242	2.2654	1.2252	1.8009	88.346	84.443
243	2.2674	1.2259	1.8016	88.387	84.461
244	2.2696	1.2268	1.8024	88.426	84.488

OD	70um (pW)	100um (pW)	160um (pW)	<T_m1> (K)	<T_m2> (K)
245	2.2723	1.2278	1.8034	88.465	84.528
246	2.2742	1.2286	1.8041	88.494	84.559
247	2.2769	1.2296	1.8051	88.543	84.589
248	2.2788	1.2303	1.8058	88.573	84.615
251	2.2869	1.2334	1.8087	88.696	84.732
252	2.2897	1.2345	1.8097	88.750	84.762
253	2.2912	1.2350	1.8103	88.770	84.786
256	2.2853	1.2328	1.8082	88.647	84.737
257	2.2868	1.2333	1.8087	88.702	84.724
258	2.2910	1.2349	1.8102	88.778	84.770
259	2.2936	1.2359	1.8111	88.817	84.808
260	2.2950	1.2365	1.8117	88.835	84.833
261	2.2965	1.2370	1.8122	88.852	84.860
262	2.2936	1.2359	1.8111	88.790	84.836
268	2.2828	1.2318	1.8072	88.635	84.670
269	2.2853	1.2328	1.8081	88.686	84.695
270	2.2867	1.2333	1.8087	88.703	84.720
271	2.2862	1.2331	1.8085	88.686	84.721
272	2.2866	1.2332	1.8086	88.697	84.721
274	2.2905	1.2347	1.8100	88.765	84.769
275	2.2915	1.2351	1.8104	88.782	84.783
284	2.2936	1.2359	1.8111	88.807	84.818
285	2.2937	1.2360	1.8112	88.815	84.815
286	2.2940	1.2361	1.8113	88.820	84.819
299	2.3009	1.2385	1.8134	88.903	84.898
300	2.2987	1.2376	1.8126	88.862	84.871
314	2.2842	1.2318	1.8070	88.619	84.635
315	2.2831	1.2314	1.8066	88.601	84.618
316	2.2825	1.2311	1.8063	88.587	84.610
320	2.2687	1.2258	1.8012	88.347	84.427
321	2.2660	1.2247	1.8002	88.303	84.388
322	2.2626	1.2234	1.7989	88.235	84.351
324	2.2597	1.2222	1.7978	88.222	84.270
325	2.2616	1.2229	1.7985	88.262	84.281
328	2.2678	1.2253	1.8007	88.348	84.370
329	2.2697	1.2259	1.8013	88.382	84.388
330	2.2722	1.2269	1.8022	88.431	84.410
343	2.2656	1.2241	1.7994	88.292	84.308
344	2.2668	1.2245	1.7998	88.309	84.322
345	2.2683	1.2251	1.8004	88.336	84.338
346	2.2679	1.2249	1.8002	88.313	84.346
347	2.2699	1.2257	1.8009	88.357	84.355
348	2.2725	1.2266	1.8018	88.402	84.383
349	2.2740	1.2272	1.8023	88.411	84.418
350	2.2755	1.2278	1.8029	88.441	84.429
351	2.2774	1.2284	1.8035	88.468	84.453
352	2.2803	1.2295	1.8045	88.518	84.485
353	2.2847	1.2312	1.8061	88.527	84.606
354	2.2793	1.2291	1.8041	88.465	84.504
355	2.2767	1.2281	1.8032	88.426	84.463
356	2.2777	1.2285	1.8035	88.464	84.450

OD	70um (pW)	100um (pW)	160um (pW)	<T_m1> (K)	<T_m2> (K)
357	2.2794	1.2291	1.8041	88.495	84.465
360	2.2836	1.2306	1.8055	88.542	84.533
361	2.2817	1.2299	1.8048	88.503	84.512
368	2.2829	1.2302	1.8050	88.516	84.508
369	2.2807	1.2293	1.8042	88.468	84.489
371	2.2779	1.2282	1.8032	88.419	84.449
372	2.2735	1.2266	1.8016	88.350	84.384
373	2.2738	1.2266	1.8016	88.366	84.371
374	2.2710	1.2256	1.8006	88.312	84.342
375	2.2706	1.2254	1.8004	88.318	84.320
376	2.2719	1.2259	1.8009	88.347	84.326
380	2.2763	1.2275	1.8024	88.393	84.396
381	2.2722	1.2259	1.8008	88.303	84.361
385	2.2661	1.2235	1.7985	88.223	84.246
386	2.2664	1.2236	1.7986	88.231	84.244
387	2.2670	1.2238	1.7988	88.241	84.246
392	2.2692	1.2245	1.7994	88.263	84.273
393	2.2698	1.2247	1.7996	88.279	84.272
394	2.2725	1.2257	1.8006	88.328	84.300
395	2.2743	1.2264	1.8012	88.347	84.329
396	2.2713	1.2252	1.8001	88.272	84.312
399	2.2694	1.2244	1.7993	88.266	84.251
400	2.2714	1.2252	1.8000	88.299	84.274
401	2.2711	1.2251	1.7999	88.274	84.289
402	2.2712	1.2251	1.7999	88.285	84.276
403	2.2718	1.2253	1.8001	88.291	84.283
404	2.2712	1.2250	1.7998	88.272	84.282
405	2.2711	1.2250	1.7998	88.271	84.278
413	2.2659	1.2228	1.7977	88.175	84.191
414	2.2626	1.2216	1.7965	88.104	84.162
415	2.2593	1.2203	1.7953	88.046	84.119
416	2.2580	1.2198	1.7947	88.044	84.077
417	2.2601	1.2206	1.7955	88.091	84.090
418	2.2618	1.2212	1.7961	88.112	84.115
420	2.2626	1.2214	1.7963	88.109	84.134
421	2.2622	1.2213	1.7962	88.102	84.127
434	2.2678	1.2231	1.7978	88.172	84.177
435	2.2631	1.2213	1.7961	88.068	84.140
436	2.2592	1.2198	1.7947	88.022	84.066
437	2.2612	1.2205	1.7953	88.074	84.068
446	2.2811	1.2280	1.8023	88.363	84.338
447	2.2818	1.2282	1.8025	88.378	84.339
448	2.2847	1.2293	1.8036	88.434	84.366
449	2.2891	1.2309	1.8051	88.509	84.416
450	2.2906	1.2315	1.8056	88.523	84.442
451	2.2920	1.2320	1.8061	88.536	84.469
452	2.2875	1.2303	1.8045	88.445	84.423
453	2.2877	1.2303	1.8045	88.460	84.411
454	2.2880	1.2304	1.8046	88.458	84.418
455	2.2878	1.2303	1.8045	88.455	84.412
456	2.2886	1.2306	1.8047	88.472	84.414

OD	70um (pW)	100um (pW)	160um (pW)	<T_m1> (K)	<T_m2> (K)
457	2.2906	1.2314	1.8054	88.511	84.431
458	2.2903	1.2312	1.8053	88.484	84.445
459	2.2909	1.2314	1.8055	88.504	84.441
460	2.2923	1.2319	1.8060	88.531	84.451
464	2.2913	1.2315	1.8055	88.495	84.444
465	2.2944	1.2326	1.8066	88.562	84.464
469	2.2915	1.2315	1.8055	88.473	84.455
470	2.2920	1.2316	1.8056	88.505	84.435
471	2.2944	1.2325	1.8064	88.551	84.453
472	2.2976	1.2337	1.8076	88.596	84.500
473	2.2994	1.2344	1.8082	88.623	84.521
474	2.3016	1.2352	1.8089	88.657	84.550
478	2.3068	1.2371	1.8107	88.725	84.621
479	2.3085	1.2377	1.8113	88.756	84.636
480	2.3112	1.2387	1.8122	88.800	84.667
481	2.3141	1.2398	1.8132	88.845	84.702
483	2.3157	1.2404	1.8138	88.846	84.744
484	2.3133	1.2394	1.8129	88.800	84.715
485	2.3131	1.2393	1.8128	88.807	84.699
486	2.3116	1.2387	1.8122	88.781	84.678
487	2.3137	1.2395	1.8130	88.825	84.692
492	2.3232	1.2430	1.8162	88.961	84.815
493	2.3239	1.2432	1.8164	88.968	84.824
497	2.3153	1.2399	1.8133	88.816	84.713
498	2.3156	1.2400	1.8133	88.832	84.700
499	2.3157	1.2400	1.8133	88.825	84.708
500	2.3143	1.2395	1.8128	88.800	84.689
501	2.3142	1.2394	1.8127	88.790	84.691
502	2.3101	1.2378	1.8112	88.713	84.645
511	2.3066	1.2363	1.8098	88.652	84.572
512	2.3043	1.2355	1.8089	88.611	84.544
513	2.3041	1.2354	1.8088	88.624	84.522
516	2.3047	1.2355	1.8089	88.627	84.523
521	2.2839	1.2275	1.8013	88.272	84.252
522	2.2887	1.2293	1.8030	88.384	84.273
528	2.2957	1.2319	1.8054	88.470	84.376
529	2.3011	1.2339	1.8073	88.571	84.428
530	2.3024	1.2344	1.8077	88.584	84.451
539	2.3075	1.2361	1.8093	88.637	84.515
540	2.3100	1.2371	1.8102	88.684	84.539
545	2.3265	1.2432	1.8160	88.947	84.740
546	2.3304	1.2446	1.8173	89.006	84.789
547	2.3340	1.2460	1.8186	89.055	84.843
553	2.3413	1.2486	1.8210	89.151	84.938
554	2.3443	1.2497	1.8221	89.201	84.974
555	2.3443	1.2497	1.8221	89.184	84.988
564	2.3425	1.2489	1.8212	89.139	84.949
565	2.3385	1.2473	1.8198	89.062	84.908
566	2.3356	1.2462	1.8187	89.015	84.865
573	2.3414	1.2482	1.8205	89.110	84.913
574	2.3423	1.2486	1.8208	89.126	84.920

OD	70um (pW)	100um (pW)	160um (pW)	<T_m1> (K)	<T_m2> (K)
575	2.3416	1.2483	1.8206	89.106	84.918
576	2.3409	1.2480	1.8203	89.094	84.904
577	2.3413	1.2481	1.8204	89.105	84.902
578	2.3439	1.2491	1.8213	89.152	84.925
579	2.3459	1.2498	1.8220	89.185	84.947
581	2.3513	1.2518	1.8239	89.258	85.026
582	2.3524	1.2522	1.8242	89.278	85.034
583	2.3549	1.2531	1.8251	89.323	85.058
584	2.3545	1.2530	1.8249	89.285	85.081
585	2.3559	1.2535	1.8254	89.323	85.079
587	2.3599	1.2549	1.8267	89.395	85.115
588	2.3655	1.2570	1.8287	89.484	85.185
589	2.3659	1.2572	1.8288	89.481	85.197
591	2.3666	1.2574	1.8291	89.477	85.216
592	2.3672	1.2576	1.8292	89.490	85.215
593	2.3671	1.2575	1.8292	89.483	85.217
599	2.3620	1.2555	1.8272	89.395	85.136
600	2.3636	1.2561	1.8277	89.427	85.147
603	2.3655	1.2568	1.8283	89.423	85.198
604	2.3664	1.2571	1.8286	89.465	85.175
605	2.3673	1.2574	1.8289	89.473	85.189
606	2.3698	1.2583	1.8298	89.518	85.214
607	2.3705	1.2585	1.8300	89.522	85.225
611	2.3739	1.2597	1.8311	89.552	85.280
612	2.3716	1.2589	1.8303	89.511	85.253
613	2.3695	1.2580	1.8295	89.474	85.225
614	2.3688	1.2578	1.8292	89.474	85.201
615	2.3680	1.2574	1.8289	89.456	85.190
616	2.3678	1.2573	1.8288	89.457	85.182
619	2.3721	1.2589	1.8302	89.523	85.228
620	2.3682	1.2574	1.8288	89.444	85.194
621	2.3670	1.2569	1.8284	89.423	85.176
627	2.3726	1.2589	1.8302	89.501	85.238
628	2.3678	1.2571	1.8285	89.417	85.179
629	2.3669	1.2567	1.8281	89.415	85.151
635	2.3714	1.2583	1.8296	89.489	85.188
636	2.3717	1.2584	1.8296	89.488	85.194
637	2.3693	1.2575	1.8288	89.432	85.178
638	2.3662	1.2563	1.8276	89.383	85.134
639	2.3603	1.2541	1.8255	89.281	85.061
640	2.3580	1.2532	1.8247	89.241	85.032
647	2.3542	1.2516	1.8231	89.186	84.950
648	2.3553	1.2520	1.8235	89.215	84.949
649	2.3565	1.2524	1.8239	89.235	84.959
651	2.3606	1.2539	1.8253	89.306	84.999
652	2.3605	1.2539	1.8252	89.285	85.017
653	2.3580	1.2529	1.8243	89.230	84.994
661	2.3603	1.2536	1.8249	89.257	85.008
662	2.3564	1.2521	1.8235	89.195	84.953
663	2.3577	1.2526	1.8239	89.233	84.946
668	2.3659	1.2556	1.8267	89.332	85.069

OD	70um (pW)	100um (pW)	160um (pW)	<T_m1> (K)	<T_m2> (K)
669	2.3664	1.2557	1.8269	89.353	85.059
670	2.3657	1.2554	1.8266	89.330	85.058
675	2.3532	1.2507	1.8220	89.129	84.882
676	2.3492	1.2491	1.8206	89.050	84.841
677	2.3460	1.2479	1.8194	89.001	84.794
684	2.3518	1.2499	1.8213	89.092	84.844
685	2.3473	1.2482	1.8196	89.005	84.799
686	2.3404	1.2456	1.8172	88.880	84.722
695	2.3365	1.2440	1.8155	88.851	84.604
696	2.3376	1.2444	1.8159	88.866	84.619
697	2.3387	1.2447	1.8162	88.884	84.628
701	2.3124	1.2348	1.8068	88.425	84.312
702	2.3163	1.2362	1.8081	88.538	84.305
703	2.3197	1.2374	1.8093	88.589	84.349
704	2.3192	1.2372	1.8091	88.550	84.372
705	2.3200	1.2375	1.8094	88.576	84.366
706	2.3214	1.2380	1.8098	88.598	84.380
712	2.3305	1.2414	1.8129	88.717	84.507
713	2.3289	1.2408	1.8124	88.687	84.489
714	2.3241	1.2389	1.8106	88.591	84.441
715	2.3197	1.2372	1.8090	88.527	84.374
716	2.3199	1.2373	1.8090	88.546	84.355
718	2.3156	1.2356	1.8075	88.468	84.301
719	2.3171	1.2362	1.8080	88.506	84.303
720	2.3181	1.2365	1.8083	88.520	84.314
721	2.3178	1.2364	1.8082	88.504	84.322
722	2.3144	1.2351	1.8070	88.433	84.290
723	2.3127	1.2345	1.8063	88.418	84.252
724	2.3128	1.2345	1.8063	88.421	84.247
725	2.3083	1.2328	1.8047	88.338	84.197
726	2.3075	1.2324	1.8044	88.327	84.182
729	2.3087	1.2328	1.8047	88.337	84.196
730	2.3070	1.2322	1.8041	88.314	84.167
731	2.3065	1.2320	1.8039	88.309	84.153
732	2.3120	1.2340	1.8058	88.418	84.197
733	2.3156	1.2353	1.8070	88.478	84.238
734	2.3205	1.2371	1.8088	88.554	84.300
737	2.3239	1.2384	1.8099	88.572	84.372
738	2.3203	1.2370	1.8086	88.499	84.339
739	2.3182	1.2362	1.8079	88.475	84.301
743	2.3323	1.2414	1.8128	88.707	84.460
744	2.3323	1.2414	1.8127	88.702	84.463
745	2.3335	1.2418	1.8131	88.720	84.474
746	2.3318	1.2412	1.8125	88.674	84.470
747	2.3277	1.2396	1.8110	88.599	84.425
748	2.3250	1.2386	1.8100	88.561	84.380
749	2.3259	1.2389	1.8103	88.590	84.373
750	2.3236	1.2380	1.8095	88.540	84.352
751	2.3227	1.2376	1.8091	88.527	84.335
757	2.3269	1.2391	1.8105	88.572	84.394
758	2.3230	1.2376	1.8091	88.504	84.344

OD	70um (pW)	100um (pW)	160um (pW)	<T_m1> (K)	<T_m2> (K)
759	2.3174	1.2355	1.8071	88.402	84.283
762	2.3060	1.2312	1.8029	88.230	84.114
763	2.3108	1.2329	1.8045	88.354	84.120
764	2.3148	1.2344	1.8059	88.416	84.170
769	2.3011	1.2292	1.8010	88.158	84.017
770	2.3027	1.2297	1.8015	88.199	84.017
771	2.3048	1.2305	1.8022	88.233	84.041
775	2.3212	1.2366	1.8080	88.476	84.260
776	2.3174	1.2352	1.8066	88.393	84.230
777	2.3136	1.2337	1.8052	88.319	84.193
780	2.3173	1.2350	1.8064	88.407	84.198
781	2.3152	1.2343	1.8057	88.357	84.187
782	2.3135	1.2336	1.8050	88.327	84.162
787	2.3249	1.2378	1.8090	88.519	84.284
788	2.3242	1.2375	1.8087	88.493	84.288
789	2.3239	1.2374	1.8086	88.493	84.275
790	2.3258	1.2381	1.8092	88.520	84.299
791	2.3242	1.2375	1.8086	88.484	84.286
792	2.3226	1.2368	1.8080	88.453	84.269
793	2.3185	1.2353	1.8066	88.384	84.215
794	2.3163	1.2344	1.8057	88.354	84.178
795	2.3155	1.2341	1.8054	88.344	84.160
797	2.3156	1.2341	1.8054	88.359	84.138
798	2.3162	1.2343	1.8056	88.360	84.152
799	2.3149	1.2338	1.8051	88.323	84.152
800	2.3090	1.2316	1.8030	88.216	84.085
801	2.3086	1.2314	1.8028	88.238	84.045
802	2.3112	1.2323	1.8037	88.285	84.067
805	2.3174	1.2346	1.8058	88.378	84.144
806	2.3214	1.2361	1.8072	88.448	84.188
807	2.3267	1.2380	1.8090	88.534	84.250
809	2.3376	1.2421	1.8129	88.688	84.404
810	2.3398	1.2429	1.8136	88.723	84.429
824	2.3310	1.2393	1.8102	88.544	84.308
825	2.3351	1.2409	1.8116	88.629	84.337
826	2.3380	1.2419	1.8126	88.670	84.374
828	2.3327	1.2399	1.8107	88.551	84.337
829	2.3375	1.2417	1.8123	88.658	84.363
830	2.3403	1.2427	1.8133	88.700	84.398
831	2.3440	1.2441	1.8146	88.753	84.450
832	2.3475	1.2454	1.8158	88.807	84.491
833	2.3526	1.2473	1.8176	88.886	84.555
842	2.3561	1.2484	1.8186	88.916	84.595
843	2.3594	1.2496	1.8197	88.970	84.633
844	2.3623	1.2507	1.8207	89.017	84.666
847	2.3703	1.2536	1.8235	89.113	84.792
848	2.3697	1.2534	1.8233	89.082	84.804
849	2.3683	1.2528	1.8227	89.073	84.766
858	2.3671	1.2522	1.8221	89.035	84.741
859	2.3680	1.2525	1.8223	89.063	84.731
860	2.3693	1.2530	1.8228	89.083	84.747

OD	70um (pW)	100um (pW)	160um (pW)	<T_m1> (K)	<T_m2> (K)
871	2.3716	1.2537	1.8233	89.092	84.768
872	2.3711	1.2534	1.8231	89.082	84.759
873	2.3686	1.2525	1.8222	89.024	84.742
887	2.3803	1.2566	1.8259	89.210	84.841
888	2.3812	1.2569	1.8262	89.224	84.851
889	2.3803	1.2565	1.8259	89.189	84.857
892	2.3718	1.2533	1.8228	89.051	84.741
893	2.3768	1.2551	1.8245	89.161	84.768
894	2.3786	1.2558	1.8251	89.186	84.791
898	2.3774	1.2553	1.8246	89.143	84.787
899	2.3798	1.2562	1.8254	89.190	84.805
900	2.3832	1.2574	1.8266	89.246	84.841
904	2.3842	1.2577	1.8268	89.248	84.854
905	2.3849	1.2580	1.8271	89.247	84.875
906	2.3849	1.2579	1.8270	89.240	84.877
909	2.3935	1.2611	1.8300	89.389	84.963
910	2.3975	1.2625	1.8313	89.445	85.016
911	2.3990	1.2630	1.8318	89.467	85.032
917	2.4092	1.2667	1.8353	89.594	85.176
918	2.4086	1.2665	1.8351	89.587	85.163
919	2.4107	1.2673	1.8358	89.626	85.181
926	2.4072	1.2658	1.8343	89.556	85.126
927	2.4046	1.2649	1.8334	89.502	85.106
928	2.4016	1.2637	1.8324	89.445	85.075
930	2.3995	1.2629	1.8316	89.416	85.037
931	2.4045	1.2647	1.8333	89.520	85.068
932	2.4069	1.2656	1.8341	89.556	85.095
934	2.4036	1.2643	1.8329	89.467	85.088
935	2.4054	1.2650	1.8335	89.525	85.076
936	2.4082	1.2660	1.8344	89.570	85.105
945	2.4196	1.2701	1.8382	89.718	85.250
946	2.4139	1.2680	1.8362	89.599	85.210
947	2.4052	1.2647	1.8331	89.446	85.112
955	2.4090	1.2659	1.8342	89.521	85.113
956	2.4092	1.2660	1.8343	89.540	85.096
957	2.4120	1.2670	1.8352	89.592	85.118
967	2.4190	1.2694	1.8374	89.675	85.200
968	2.4181	1.2691	1.8371	89.648	85.200
969	2.4184	1.2692	1.8371	89.661	85.191
973	2.4242	1.2712	1.8391	89.732	85.271
974	2.4219	1.2704	1.8382	89.689	85.247
975	2.4226	1.2706	1.8384	89.718	85.231
981	2.4156	1.2678	1.8358	89.606	85.122
982	2.4176	1.2686	1.8365	89.637	85.146
983	2.4196	1.2693	1.8371	89.666	85.168
1000	2.4163	1.2678	1.8356	89.557	85.130
1001	2.4134	1.2667	1.8345	89.508	85.093
1002	2.4107	1.2656	1.8336	89.468	85.053
1005	2.4160	1.2675	1.8353	89.581	85.074
1006	2.4205	1.2692	1.8368	89.648	85.130
1007	2.4235	1.2703	1.8379	89.694	85.167

OD	70um (pW)	100um (pW)	160um (pW)	<T_m1> (K)	<T_m2> (K)
1026	2.4189	1.2682	1.8358	89.566	85.103
1027	2.4133	1.2661	1.8338	89.462	85.048
1028	2.4103	1.2650	1.8327	89.411	85.009
1034	2.4030	1.2621	1.8300	89.319	84.870
1035	2.4035	1.2623	1.8301	89.324	84.875
1036	2.4034	1.2622	1.8301	89.315	84.878
1037	2.4019	1.2617	1.8295	89.290	84.858
1038	2.4015	1.2615	1.8294	89.288	84.847
1039	2.4011	1.2613	1.8292	89.276	84.841
1040	2.3999	1.2608	1.8288	89.259	84.822
1041	2.3970	1.2598	1.8278	89.194	84.805
1042	2.3926	1.2581	1.8262	89.115	84.755
1043	2.3894	1.2569	1.8250	89.086	84.688
1044	2.3887	1.2566	1.8247	89.081	84.670
1045	2.3892	1.2568	1.8249	89.090	84.670
1049	2.3876	1.2561	1.8243	89.029	84.676
1050	2.3856	1.2553	1.8235	89.012	84.630
1051	2.3849	1.2551	1.8232	89.004	84.614
1057	2.3841	1.2546	1.8228	89.008	84.564
1058	2.3867	1.2556	1.8237	89.044	84.599
1059	2.3877	1.2560	1.8240	89.046	84.625
1063	2.3912	1.2572	1.8251	89.088	84.668
1064	2.3903	1.2568	1.8248	89.067	84.661
1065	2.3888	1.2562	1.8242	89.035	84.647
1074	2.3844	1.2544	1.8224	88.978	84.545
1075	2.3827	1.2538	1.8218	88.928	84.548
1076	2.3786	1.2522	1.8204	88.847	84.509
1081	2.3850	1.2545	1.8225	88.954	84.567
1082	2.3767	1.2514	1.8196	88.789	84.496
1083	2.3696	1.2488	1.8170	88.690	84.387
1095	2.3922	1.2569	1.8247	89.023	84.655
1096	2.3905	1.2563	1.8241	88.992	84.637
1101	2.3827	1.2533	1.8212	88.896	84.490
1102	2.3869	1.2548	1.8226	88.962	84.539
1103	2.3867	1.2547	1.8225	88.954	84.536
1108	2.3879	1.2550	1.8228	88.968	84.540
1109	2.3909	1.2561	1.8238	89.021	84.567
1110	2.3925	1.2567	1.8243	89.043	84.589
1119	2.3732	1.2494	1.8174	88.687	84.372
1120	2.3715	1.2487	1.8167	88.685	84.320
1121	2.3715	1.2487	1.8167	88.691	84.309
1122	2.3714	1.2487	1.8167	88.687	84.308
1123	2.3716	1.2487	1.8167	88.691	84.305
1124	2.3720	1.2488	1.8168	88.695	84.308
1136	2.3689	1.2475	1.8154	88.632	84.243
1137	2.3688	1.2474	1.8153	88.624	84.246
1138	2.3678	1.2470	1.8150	88.599	84.238
1139	2.3661	1.2464	1.8144	88.560	84.229
1146	2.3684	1.2471	1.8150	88.596	84.232
1147	2.3662	1.2463	1.8142	88.552	84.212
1148	2.3639	1.2454	1.8134	88.515	84.179

OD	70um (pW)	100um (pW)	160um (pW)	<T_m1> (K)	<T_m2> (K)
1157	2.3689	1.2471	1.8149	88.606	84.197
1158	2.3703	1.2475	1.8153	88.621	84.219
1159	2.3722	1.2482	1.8160	88.651	84.239
1170	2.3754	1.2492	1.8168	88.662	84.283
1171	2.3774	1.2499	1.8175	88.709	84.287
1172	2.3816	1.2514	1.8189	88.782	84.327
1179	2.3775	1.2498	1.8173	88.688	84.285
1180	2.3804	1.2509	1.8183	88.742	84.308
1181	2.3837	1.2521	1.8194	88.799	84.340
1182	2.3884	1.2538	1.8210	88.864	84.404
1183	2.3917	1.2550	1.8221	88.908	84.452
1184	2.3936	1.2557	1.8228	88.937	84.473
1193	2.3993	1.2577	1.8246	88.986	84.559
1194	2.3942	1.2558	1.8228	88.889	84.510
1195	2.3906	1.2544	1.8215	88.840	84.453
1196	2.3930	1.2552	1.8223	88.908	84.445
1197	2.3953	1.2561	1.8231	88.935	84.481
1198	2.3957	1.2562	1.8232	88.933	84.489
1200	2.4001	1.2578	1.8247	88.998	84.543
1201	2.3985	1.2572	1.8241	88.960	84.534
1202	2.3966	1.2565	1.8234	88.930	84.507
1214	2.4165	1.2636	1.8300	89.213	84.745
1215	2.4125	1.2621	1.8286	89.140	84.703
1216	2.4103	1.2613	1.8278	89.112	84.664
1235	2.3977	1.2562	1.8229	88.919	84.435
1236	2.4024	1.2579	1.8245	88.998	84.482
1237	2.4066	1.2595	1.8259	89.049	84.547
1244	2.4081	1.2599	1.8263	89.036	84.581
1245	2.4092	1.2603	1.8266	89.064	84.579
1246	2.4122	1.2614	1.8276	89.118	84.604
1249	2.4098	1.2605	1.8268	89.059	84.590
1250	2.4130	1.2616	1.8278	89.127	84.605
1251	2.4179	1.2634	1.8295	89.204	84.660
1264	2.4185	1.2634	1.8294	89.184	84.655
1265	2.4228	1.2649	1.8308	89.257	84.697
1266	2.4269	1.2664	1.8322	89.317	84.748
1270	2.4178	1.2630	1.8290	89.158	84.641
1271	2.4231	1.2649	1.8308	89.253	84.689
1272	2.4276	1.2666	1.8323	89.325	84.739
1273	2.4343	1.2690	1.8346	89.416	84.832
1274	2.4380	1.2704	1.8359	89.466	84.884
1275	2.4407	1.2713	1.8368	89.503	84.920
1279	2.4527	1.2757	1.8409	89.670	85.076
1280	2.4500	1.2747	1.8399	89.604	85.065
1281	2.4449	1.2728	1.8381	89.505	85.022
1285	2.4527	1.2756	1.8407	89.670	85.052
1286	2.4550	1.2764	1.8414	89.698	85.086
1287	2.4543	1.2761	1.8412	89.670	85.092
1293	2.4638	1.2795	1.8443	89.814	85.191
1294	2.4653	1.2800	1.8448	89.835	85.209
1295	2.4656	1.2801	1.8449	89.833	85.215

OD	70um (pW)	100um (pW)	160um (pW)	<T_m1> (K)	<T_m2> (K)
1308	2.4607	1.2781	1.8428	89.741	85.127
1309	2.4616	1.2784	1.8431	89.752	85.137
1310	2.4618	1.2785	1.8432	89.750	85.144
1314	2.4601	1.2777	1.8425	89.714	85.118
1315	2.4573	1.2767	1.8415	89.659	85.092
1316	2.4533	1.2752	1.8401	89.590	85.050
1317	2.4513	1.2745	1.8394	89.559	85.021
1320	2.4438	1.2716	1.8367	89.466	84.892
1321	2.4446	1.2719	1.8369	89.476	84.899
1322	2.4445	1.2719	1.8369	89.462	84.909
1327	2.4387	1.2696	1.8347	89.385	84.804
1328	2.4415	1.2706	1.8357	89.431	84.834
1329	2.4465	1.2724	1.8374	89.512	84.886
1332	2.4526	1.2746	1.8394	89.578	84.982
1333	2.4553	1.2756	1.8403	89.628	85.004
1334	2.4573	1.2763	1.8410	89.655	85.028
1337	2.4610	1.2776	1.8422	89.696	85.082
1338	2.4605	1.2774	1.8420	89.687	85.074
1339	2.4616	1.2778	1.8423	89.705	85.083
1344	2.4664	1.2795	1.8438	89.765	85.138
1345	2.4655	1.2791	1.8435	89.744	85.133
1346	2.4645	1.2788	1.8432	89.725	85.120
1349	2.4657	1.2791	1.8435	89.741	85.128
1350	2.4655	1.2790	1.8434	89.740	85.119
1351	2.4637	1.2784	1.8428	89.698	85.109
1354	2.4622	1.2777	1.8421	89.696	85.056
1355	2.4638	1.2783	1.8427	89.714	85.080
1356	2.4655	1.2789	1.8432	89.742	85.095
1375	2.4593	1.2763	1.8406	89.597	85.007
1376	2.4579	1.2758	1.8401	89.572	84.990
1377	2.4548	1.2746	1.8390	89.523	84.948
1378	2.4536	1.2741	1.8386	89.510	84.923
1379	2.4522	1.2736	1.8381	89.491	84.900
1380	2.4533	1.2740	1.8384	89.519	84.897
1399	2.4612	1.2765	1.8407	89.585	84.989
1400	2.4559	1.2746	1.8388	89.486	84.941
1401	2.4527	1.2734	1.8377	89.430	84.904
1402	2.4397	1.2685	1.8332	89.254	84.713
1403	2.4416	1.2692	1.8338	89.303	84.710
1404	2.4440	1.2701	1.8346	89.344	84.731
1418	2.4340	1.2661	1.8308	89.140	84.616
1420	2.4338	1.2660	1.8307	89.150	84.591
1426	2.4330	1.2656	1.8302	89.122	84.576
1427	2.4329	1.2655	1.8302	89.127	84.564
1428	2.4342	1.2660	1.8306	89.150	84.572
1440	2.4403	1.2680	1.8324	89.216	84.639
1441	2.4407	1.2681	1.8325	89.219	84.642
1442	2.4402	1.2680	1.8323	89.209	84.635
1443	2.4395	1.2677	1.8320	89.198	84.622
1444	2.4385	1.2673	1.8317	89.175	84.616
1445	2.4369	1.2667	1.8311	89.146	84.597